



HiWaQ v1.0: A flexible catchment water quality assessment tool with compatibility for multiple hydrological model structures

Xiaoqiang Yang^{1,2}, Doerthe Tetzlaff^{2,3,4}, Chris Soulsby^{4,2}, Dietrich Borchardt¹

¹Department of Aquatic Ecosystem Analysis and Management, Helmholtz Centre for Environmental Research – UFZ,
Magdeburg, 39114, Germany

²Department of Ecohydrology and Biogeochemistry, Leibniz Institute of Freshwater Ecology and Inland Fisheries (IGB),
Berlin, 12587, Germany

³Department of Geography, Humboldt University of Berlin, Berlin, 10117, Germany

⁴Northern Rivers Institute, School of Geosciences, University of Aberdeen, Aberdeen, AB24 3UF, UK

Correspondence to: Xiaoqiang Yang (xiaoqiang.yang@ufz.de)

Abstract. Mitigating diffuse-source nutrient pollution has created an urgent need to advance understanding of catchment hydrological and nutrient dynamics, and develop robust integrated hydrological and water quality models to support decision making. However, the current availability of integrated catchment-scale water quantity and quality assessment tools is very limited compared to that of hydrological models, and the common developing strategy of extending existing hydrological platforms might be restricted by specific hydrological structures and associated data requirements. Here we introduce a new flexible catchment water quality assessment tool – HiWaQ that aims to be compatible with multiple, often contrasting hydrological model structures and that comprehensively considers spatio-temporally varying water quality impacts of anthropogenic activities. The flexibility of HiWaQ is realised through: (1) a unified configuration interface for catchment characteristics and the coupled hydrological structure; and (2) a generalised structure of storage-flux interactions for all bucket-type storages. We also present the detailed N module development (HiWaQ-N) for nitrate simulation and its coupling tests with two contrasting fully distributed hydrological models (the process-based ecohydrological EcH₂O-iso model and the multi-scale conceptual mHM model). The two couplings were tested and cross-compared in the mixed forest-agricultural Silberhütte catchment (99 km²), central Germany, using the continuous daily discharge and Nitrate-N observations over 2012-2018. Results demonstrated that: (1) HiWaQ-N could well reproduce the observed discharge and stream Nitrate-N patterns and provided reliable spatio-temporal estimates of catchment N balance and networked in-stream N retention; (2) the two couplings were generally consistent with each other, while they showed subtle, but insightful differences in N transport (e.g., responses to small summer rainfall events) and transformations (e.g., the soil denitrification process), which could be attributed largely to different hydrological structures. Despite promising potential for further exploiting the coupled catchment modelling (e.g., combining in-depth uncertainty analysis), HiWaQ has the unique value of making better use of advanced hydrological modelling that embeds thoughtful modelling workflows and localised perceptual knowledge, thus better leveraging these advancements in the integrated catchment water quantity-quality assessments. We encourage interested researchers and



modellers to contribute to further open-source development, which is oriented to be scientifically insightful and practically useful for catchment management.

1 Introduction

35 Maintenance of good water quality is a key aspect of hydrologic ecosystem services (Brauman, 2015) and essentially effects the provision of other services, such as recreation and sustaining human health (Keeler et al., 2012). Increasing anthropogenic demands and climate change pressures have amplified challenges to water-related ecosystem services (Millennium Ecosystem Assessment, 2005; Guswa et al., 2014; Brauman, 2015). Among others, anthropogenically sourced nutrients have been substantially threatening ecosystem functioning of fresh- and marine water systems (Rockström et al., 2009). The plateaued, 40 though still excessive nutrient levels are largely ascribed to agricultural diffuse sources (Kroon et al., 2016; Reusch et al., 2018; Van Meter et al., 2018). Further control and mitigation require a solid scientific understanding of water and solute dynamics at the catchment scale, and based on this, developing robust, integrated hydrological and water quality models to support decision making (Guswa et al., 2014; Wellen et al., 2015; Jawitz et al., 2020).

Integration between hydrology and water quality at catchment scale has been attempted for many years (e.g., Rode et al., 2010; 45 Soulsby et al., 2002; Tscheikner-Gratl et al., 2019; Wellen et al., 2015). However, there still exist considerable disconnections between the two modelling communities, which tend to focus on either water quantity or water quality predictions. For example, processes are largely formulated adequately in their respective models, whilst these lack holistic and consistent interaction formulations based on integrations of interdisciplinary expertise (Hrachowitz et al., 2016). Further, advanced process-based hydrological models comprise a wide range of tools targeting various spatial and temporal scales with different 50 degrees of complexity in process representation (Clark et al., 2017a). However, in comparison, models facilitating catchment-scale water quality assessment are relatively limited. For example, Wellen et al. (2015) found that the spatially distributed, process-based catchment water quality modelling field is dominated by only five models (i.e., SWAT (Arnold et al., 1998), INCA (Wade et al., 2002), AGNPS/AnnAGNPS (Young et al., 1989), HPSF (Bicknell et al., 1997) and HBV/HYPE (Andersson et al., 2005; Lindström et al., 2010), accounting for more than 80% of 257 investigated scientific publications).

55 Nutrient transport across catchment landscapes is principally driven by hydrological flux dynamics, meanwhile, associated biogeochemical transformations are related to relative exposure and reaction timescales (Oldham et al., 2013; Li et al., 2021). These intrinsic interactions primarily lead to the fact that water quality process formulations are usually deeply integrated within specific hydrological model structures; indeed, recent catchment water quality models are mostly developed in the way of extending an existing hydrological modelling platform (e.g., mHM-Nitrate (Yang et al., 2018) and BioRT-Flux-PIHM (Zhi et al., 2022)). Although such a developing strategy can make use of advanced features of integrated hydrological platforms, 60 the applicability and transferability are somewhat restricted by specific hydrological structures and their data requirements (Norling et al., 2021). We argue that there remains a strong need to develop flexible water quality assessment tools that are compatible with various (eco-) hydrological structures and can facilitate simultaneous catchment-scale water quantity and



quality assessments. Such new flexible water quality assessment tools should take advantages of available eco-hydrological
 65 modelling structures, acting as an alternative moving toward environmental models of everywhere (Beven, 2007). Meanwhile,
 for a specific catchment, they can enable cross-comparisons of different hydrological process representations and further
 investigate their impacts on nutrient dynamics, enriching insights into holistic catchment water quantity and quality
 functioning.

The general characteristics of process-based water quality modelling provide the opportunity of developing such a flexible,
 70 widely compatible assessment tool. For example, reaction rates of nutrient transformations are often quantified based on first-
 order or Michaelis–Menten kinetics (Li et al., 2021; Reichert et al., 2001), with model parameters introduced for poorly
 understood interaction mechanisms and empirical functions employed for influences of environmental controls (Yang et al.,
 2019b). Moreover, nutrient storage-flux interactions in each bucket-type storage commonly follow the law of mass balance
 and full-mixing assumptions, with additional passive storage might be influential in attenuating solute dynamics (Wade et al.,
 75 2002; Birkel et al., 2011; Yang et al., 2018; Shanahan et al., 2001). However, the key challenges are to incorporate significant
 differences in hydrological structures associated with various, often contrasting process-based catchment models (Gupta et al.,
 2012), including (1) different catchment discretization schemes (e.g., semi- or fully distributed models) and drainage
 configurations (lateral hydrological connectivity via channel routing and/or terrestrial drainage) and (2) different
 conceptualisations and formulations of hydrological processes.

80 Here we developed a new water quality assessment tool – HiWaQ that is compatible with various hydrological structures and
 present a detailed implementation of the Nitrogen module (HiWaQ-N). This development leverages benefits from existing
 advanced catchment (eco-) hydrological models and can facilitate synthetic water resources assessments in terms of quantity
 and quality in a technically easier way. The flexibility of HiWaQ-N was tested through coupling with two contrasting grid-
 based catchment models, specifically, the process-based ecohydrological model EcH2O-iso and the multi-scale conceptual
 85 hydrological model mHM, representing both different process conceptualisations and spatial representations of the catchment
 heterogeneity. The model performance of nitrate-nitrogen ($NO_3^- - N$) simulations and cross-comparisons between the two
 couplings were evaluated in the mixed forest-agriculture Silberhütte catchment (99 km²), central Germany. The objectives of
 this paper are (1) to comprehensively introduce the HiWaQ structural design and its coupling interface, (2) based on the
 HiWaQ-N model development and its coupling with EcH2O-iso and mHM, to demonstrate the flexibility of the new platform
 90 and test the model capability of simulating $NO_3^- - N$, and (3) based on cross-comparisons between the two model couplings,
 to evaluate effects of contrasting hydrological conceptualisations on spatio-temporal variability of catchment N dynamics. As
 a model description paper, we further summarized the flexibility and strength of the HiWaQ platform, as well as its limitations
 and outlook, which are anticipated to motivate interested researchers to contribute to future open-source development.



2 The HiWaQ Overview and the nitrogen module development

95 2.1 HiWaQ design and coupling structures

HiWaQ was developed to provide a generalised tool that can easily facilitate catchment water quality assessments across spatio-temporal scales, in accordance with readily available, pre-existing hydrological modelling frameworks. This means that the new tool needs to be compatible with various process-based hydrological simulators (currently restricted to one-dimensional ordinary differential equations - ODEs for water movement), independent from catchment configuration schemes (e.g., semi- and fully distributed treatments, **Fig. 1a**) and hydrological model structures (e.g., different hydrological domains and flow paths, **Fig. 1b**). The HiWaQ tool realises the coupling via a unified interface, where catchment and modelling settings are specified (**Figure 1c**, and detailed examples of the configuration file “wqm_config.nml” in the repository Yang et al. (2022b)). Here, we briefly describe some of the relevant coupling settings:

- 105 *Catchment discretisation and landscape heterogeneity.* HiWaQ requires explicit specification of the coupled hydrological model type (“*model_type*”: “1” for grid-based fully distributed and “2” for semi-distributed types), as catchment inputs (catchment geographic characteristics and climate forcing data) and hydrological modelling outputs (internal state variables and fluxes) are always organised differently. Importantly, the two model types represent landscape heterogeneity in different ways, which requires different input information and file formats. The semi-distributed type is relatively straightforward with the hierarchical structure of subdividing into sub-catchments and HRUs, thus, HiWaQ requires only areal proportions of HRUs in each sub-catchment. For the fully distributed type, spatial distributions of landuse and soil types at the spatial resolution of the modeling are required; moreover, spatial heterogeneity is further considered by allowing multiple types to be present in one grid cell, given that their areal proportions are also provided. At each time step, HiWaQ updates vertical nutrient fluxes and storage states, looping through all basic calculation units (i.e., HRUs of all sub-catchments for semi-distributed and grid cells for fully distributed types). For the semi-distributed modeling, these state variables are averaged with weights of HRU areal proportions of each sub-catchment, resulting in total terrestrial-phase fluxes and storage states; whereas for fully distributed modeling, such aggregations are not needed, except when the spatial resolution of routing calculation is coarser than that of the terrestrial calculation.
- 120 *Drainage network and hillslope-channel configuration.* HiWaQ further considers lateral exchanges across a catchment, following its topographic drainage network. For the semi-distributed modeling in HiWaQ, the lateral exchange is only possible through stream channel routing at the sub-catchment level. Thus, aggregated information on the network morphology, such as the routing sequence of all sub-catchments and total stream length in each sub-catchment, is sufficient. There is an option to distinguish between local streams (that take sub-catchment terrestrial exports as input) and main streams (that take the routed outputs from local streams and upstream sub-catchments as input) for higher-order sub-catchments. For the fully distributed modeling, lateral exchanges are possible for different hydrological domains (e.g., surface overland flow, groundwater flow and deeper baseflow), as well as the stream



channel routing. The terrestrial-channel organization for fully distributed modeling is further flexibly implemented: (1) when terrestrial lateral exchange is enabled, the channel domain can be independently specified based on the real-world river network (i.e., only channel-connected grid cells involve stream routing processes); (2) the channel routing resolution can be set differently from that of terrestrial modeling resolution. HiWaQ requires spatially distributed drainage information for each grid cell at the routing resolution, including the geographic location, major flow direction according to topography, total stream length and average stream width. The computing order and grid organization are automatically resolved based on the supplied geographic and topographic information (e.g., the headwater grid cells should be computed prior to higher-order grid cells).

- Hydrological compartments and processes.* Despite differences in catchment treatments and configurations, usually process-based models conceptualise hydrological processes and storage-flux interactions within the basic calculation units in a similar way, that is, defining multiple bucket-type reservoirs for water storages in different hydrological compartments and multiple input-output fluxes for water exchanges between hydrologically connected compartments and atmospheric interactions (mainly rainfall or snowfall inputs and evapotranspiration outputs). As illustrated in **Figure 1b**, HiWaQ currently implements a comprehensive suite of hydrological compartments (i.e., canopy interception, snowpack, surface water ponding, impermeable urban surface, soil water, groundwater, deep groundwater and stream surface water;) and processes at vertical (i.e., canopy-exceeding throughfall, snowpack accumulation and snowmelt, surface infiltration and downward transport between different soil layers, recharge to gravitationally free groundwater storage, percolation to deeper groundwater system, canopy and soil evaporation, vegetation transpiration) and lateral (i.e., stream runoff generation via surface overland flow, subsurface flow, deeper baseflow, direct runoff from impervious surface and point sources from urban areas; terrestrial exchanges via surface, subsurface and deeper groundwater system, and consequent vertical surface run-on re-infiltration and upward return flows) directions. Note that HiWaQ considers the temporary surface water ponding only for surface runoff generations, and structures for surface lakes and reservoirs are not implemented yet.
- Flow paths and storage-flux interactions.* In accordance with the specific coupled hydrological structure, the activated hydrological compartments and processes should be turned on explicitly in the interface (i.e., “*processCase*”), and HiWaQ will run quality checks ensuring (1) associated variable names of storages and fluxes are provided in the interface; and (2) computed values from the external hydrological modelling are supplied and correctly formatted. For the generalisation of storage-flux interactions of various hydrological compartments, HiWaQ designs a generalised bucket-type storage structure (**Figure 1c**), where all possible input-output fluxes (i.e., four vertical and two lateral connections to other hydrological compartment storages, as well as any additional fluxes) can be specified. Such a structure applies to both physical storage (e.g., soil water storages at different layers) and conceptual storage (e.g., the so-called “unsaturated storage” of the HBV model (Bergström, 1995)). For the latter, it is worth noting that (1) an additional variable pointing to one physical storage as the source water is required; and (2) if its “*up_in*” flux is not specified (i.e., equals the default “none”), HiWaQ will directly replace the solute concentration of the conceptual



storage with that of its source storage, otherwise normal full mixing calculation is applied. HiWaQ reads in all externally simulated hydrological information as the NetCDF format (Unidata, 2022).

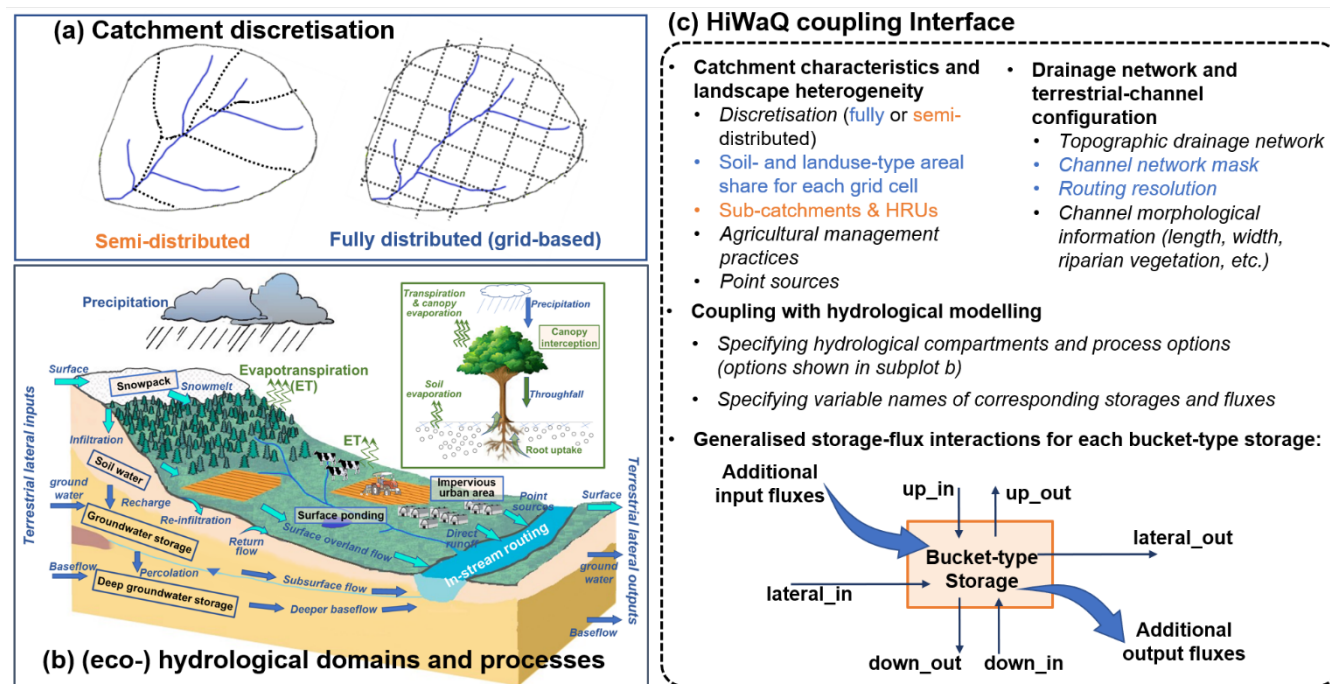


Figure 1. The flexibly designed water quality assessment tool HiWaQ for various (eco-)hydrological modelling with different catchment discretisation schemes (a) and hydrological compartments and processes (b). The coupling is realised through a unified interface (c). The background picture in (b) is adapted from National Academies of Sciences, Engineering and Medicine (2018). Note that (b) only demonstrates a schematic structure, where actual storages and their storage-flux interactions depend on the coupled hydrological models and should be specified in the coupling interface. Andersson, L., Rosberg, J., Pers, B. C., Olsson, J., and Arheimer, B.: Estimating Catchment Nutrient Flow with the HBV-NP Model: Sensitivity to Input Data, *Ambio*, 34, 521–532, 2005.

2.2 Anthropogenic impacts and nutrient transformation parameterisation

In addition to the nutrient transport driven by hydrological dynamics, anthropogenic nutrient inputs from urban point sources and agricultural diffuse sources can significantly elevate nutrient levels in freshwater and marine waters, threatening safe-operations of ecosystems (Rockström et al., 2009). Following the advanced implementations in the mHM-Nitrate model (Yang et al., 2018; Yang and Rode, 2020), HiWaQ facilitates comprehensive consideration of spatio-temporal variability of anthropogenic impacts. For fully distributed modelling, point-source inputs, whenever available, can be placed at the grid cells where, for example, sewage plants are exactly located (see “&gaugenetwork” section of the configuration file), and the heterogeneity of cropping systems is well represented by spatial maps of rotation types (similar to the representation of landuse heterogeneity) and crop sequences for each type (a look-up-table file specified for “fn_lut_rotation” in the configuration file). Detailed crop and management information (nutrient uptake, fertilization management and farming dates for each crop) is



provided via a look-up-table (file name specified for “*fn_cropinfo*” in the configuration file). Notably, the same crop with different management practices (e.g., different fertilizer application rates or farming dates) can be defined separately with different crop IDs and placed at different spatial locations via rotation maps. For semi-distributed modelling, point source inputs are added at the sub-catchment level after aggregating terrestrial exports from different HRUs, and only one set of crops and their rotation sequence is allowed for one sub-catchment.

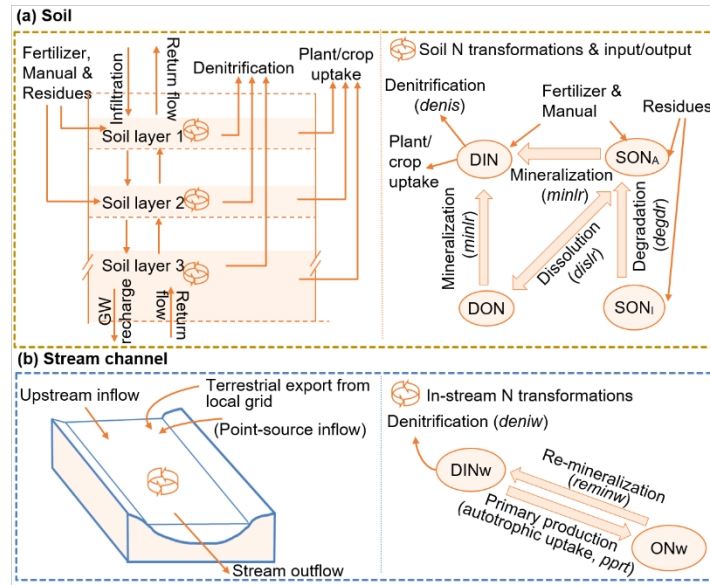
Parameters representing nutrient transformations are parsimoniously introduced in HiWaQ. The model conceptualisation of nutrient biogeochemical reaction rates consists of resolving environmental factors based on widely accepted empirical functions (e.g., quantifying temperature effects using the Q_{10} coefficient (Stanford et al., 1975)) and encapsulating all other unclear impacts as model parameters (to be calibrated in specific catchments). These parameters are often further tied to landscape categories (e.g., landuse or soil types (Clark et al., 2017b; Jawitz et al., 2020)). HiWaQ facilitates flexible parameterisation schemes, i.e., (1) the users can separately specify landscape dependency for each parameter (currently as either landuse or soil type dependent), and (2) the category types can be further grouped into several groups to reduce the total parameter numbers (see details in Yang et al. (2022b)).

2.3 Descriptions of N transport and biogeochemical transformations in HiWaQ-N

Based on the HiWaQ tool, the catchment nitrate model HiWaQ-N was developed from the mHM-Nitrate v2.0 model (Yang et al., 2018; Yang and Rode, 2020). Here, we provide brief descriptions of the N dynamics and transformation implementations. Along with hydrological dynamics across the catchment (e.g., **Figure 1b**), each water flux is associated with a $NO_3^- - N$ concentration, and each bucket-type storage updates its $NO_3^- - N$ storage and concentration based on the full mixing of input fluxes and the previous-step storage. Nitrogen biogeochemical transformations are considered only in soil water storage at different soil layers and in the stream water storage (**Figure 2**). $NO_3^- - N$ concentrations of the output fluxes of each storage are directly assigned as the updated concentration after the mixing and, if applicable, biogeochemical transformations.

In the terrestrial phase (**Figure 2a**), initially adapted from the HYPE model (Lindström et al., 2010), soil N of each layer is differentiated in four forms (dissolved inorganic nitrogen – DIN; dissolved organic nitrogen – DON; active and inactive solid organic nitrogen – SON_A and SON_I , respectively), and transformations among these N pools are considered, including denitrification removal of DIN (exclusively $NO_3^- - N$ in this study), mineralization from DON and SON_A to DIN, dissolution between DON and SON_A , and degradation from SON_I to SON_A . External N inputs from fertilizer/manure application and plant residues are added into corresponding soil N pools, while only partitioned between the first-two soil layers, with the depth of ~0-0.5 m as the major root zone. Crop/plant N uptake is calculated following two steps: (1) the potential N uptake of each crop/vegetation type is estimated firstly using a three-parameter logistic grow function and partitioned between the first three soil layers (depth up to ~2.0 m as the maximum rooting depth), (2) then, the actual N uptake from each soil layer is further constrained by soil water and soil N availabilities. In the in-stream phase (**Figure 2b**), stream water dissolved inorganic nitrogen (DIN_w , exclusively $NO_3^- - N$ in this study) and organic nitrogen (ON_w) pools are considered, with transformations of in-stream denitrification removal, autotrophic uptake as primary production and re-mineralization. Brief descriptions of

these biogeochemical transformations and corresponding reaction rates (introduced as HiWaQ-N parameters) are provided in
 215 **Table 1**, and for details of empirical functions of the abiotic environmental factors, please refer to the source code (Yang et
 al., 2022b), as well as the online documents from the HYPE model
 (http://www.smhi.net/hype/wiki/doku.php?id=start:hype_model_description, last access 23th September, 2022).



220 **Figure 2.** N dynamics and biogeochemical transformations in soil (a, exemplated as three soil layers) and in-stream (b) phases. Dissolved inorganic nitrogen – DIN; dissolved organic nitrogen – DON; active and inactive solid organic nitrogen – SON_A and SON_I, respectively; stream water dissolved inorganic nitrogen – DIN_w and organic nitrogen – ON_w. Transformation equations and parameters (italic parenthesized abbreviations) are described in Table 1.

225 **Table 1.** Descriptions of Nitrogen transformations, governing equations and introduced parameters. Please refer to the source code (Yang et al., 2022b) for details of the empirical functions quantifying abiotic environmental factors (i.e., $f_{soiltemp}$ -soil temperature, f_{sm_deni} -soil moisture specifically for denitrification, f_{sm} -soil moisture, f_{smc} -soil water nitrate concentration, $f_{watertemp}$ -stream water temperature for in-stream denitrification, $f_{waterconc}$ -stream water nitrate concentration, f_{GR} -global radiation, f_{LAI} -riparian vegetation leaf area index, f_{tempm} -stream water temperature for the inversing primary production and mineralization, and f_{tp} - long-term average total phosphorus concentration) . A and H denote stream benthic area and water depth of each stream segment, respectively.

Transformation	Description	Governing equation	Parameter
Denitrification	Removal ($DENI$) of soil DIN due to denitrification process	$DENI = denis \cdot f_{soiltemp} \cdot f_{sm_deni} \cdot f_{smc} \cdot DIN$	Denitrification rate $denis$ (d^{-1})
Mineralization	Mineralization from SON _A and DON pools to DIN	$TRANS1 = minlr \cdot f_{soiltemp} \cdot f_{sm} \cdot SON_A$ $TRANS2 = minlr \cdot f_{soiltemp} \cdot f_{sm} \cdot DON$	Mineralization rate $minlr$ (d^{-1})
Dissolution	Dissolution from SON _A to DON	$TRANS = dislr \cdot f_{soiltemp} \cdot f_{sm} \cdot SON_A$	Dissolution rate $dislr$ (d^{-1})



Degradation	Degradation from SON_I to SON_A	$TRANS = degdr \cdot f_{soiltemp} \cdot f_{sm} \cdot SON_I$	Degradation rate $degdr$ (d^{-1})
In-stream denitrification	Permanent nitrate removal ($DENI_w$) in stream water due to denitrification process	$DENI_w = \min(0.5 \cdot DIN_w, deniw \cdot f_{watertemp} \cdot f_{waterconc} \cdot A)$	In-stream denitrification rate $deniw$ ($kg\ m^{-2}\ d^{-1}$)
In-stream gross assimilation and remineralization (Yang et al., 2019a)	Gross nitrate assimilation ($ASSI_w$) for in-stream primary production and net assimilation ($NetASSI$) because part of $ASSI_w$ is returned due to remineralization	$ASSI_w = \min(0.9 \cdot DIN_w, U_{a,max} \cdot f_{GR} \cdot (1 - f_{LAI}) \cdot A)$ $NetASSI = \min(0.5 \cdot DIN_w, npprt \cdot f_{tempm} \cdot ASSI_w)$	In-stream gross assimilatory uptake rate $U_{a,max}$ ($kg\ m^{-2}\ d^{-1}$) and net assimilation proportion $npprt$ (-) after the remineralization
In-stream net assimilation or net mineralization (Lindström et al., 2010)	Generic approach for either net primary production or net mineralization release (originally implemented in HYPE)	$NetASSI = \min(0.5 \cdot DIN_w, wprod \cdot f_{tempm} \cdot f_{tp} \cdot H \cdot A)$	generic parameter $wprod$ ($kg\ m^{-3}\ d^{-1}$) representing in-stream production/decay

230

3 The HiWaQ-N coupling tests and cross-comparisons

The HiWaQ-N coupling tests were conducted using the process-based ecohydrological EcH₂O-iso model (Maneta and Silverman, 2013; Kuppel et al., 2018a) and the conceptual hydrological mHM model (Samaniego et al., 2010). Given the substantial differences between the two models (see below subsections and **Table S1**), these tests allow testing of the flexibility of the HiWaQ tool in coupling with contrasting hydrological process conceptualisations and representations of catchment heterogeneity. Moreover, the two coupled $NO_3^- - N$ simulations could be validated using continuous daily discharge and $NO_3^- - N$ observations in the mixed forest-agriculture Silberhütte catchment and cross-compared to unravel spatio-temporal variability of catchment flow and N dynamics, as well as their interactions.

235

3.1 Testing model 1: the ecohydrological EcH₂O-iso model

EcH₂O-iso is a fully distributed, process-based ecohydrological model, which integrates modules of energy balance, water balance, vegetation dynamics and flux tracking based on stable isotopes of water (Maneta and Silverman, 2013; Kuppel et al., 2018a; Smith et al., 2021). For each grid cell, the energy balance is solved at the vegetation canopy and the land surface levels, simulating soil-vegetation-atmosphere energy dynamics. Latent heat fluxes due to canopy evaporation and soil evaporation are constrained by the water availability in the intercepted storage and first-layer soil water storage, respectively. Transpiration associated latent heat flux is further controlled by the canopy conductance. A Jarvis-type model is used for calculating stomatal conductance (Jarvis, 1976), considering vegetation-dependent maximum physiological stomatal conductance and effects of environmental factors (solar radiation, air temperature, vapor pressure deficit and available soil moisture). Then, leaf area

245



index is used to scale the stomatal conductance to canopy conductance. The transpiration flux is partitioned into three soil layers, according to root distributions (determined by an exponential function (Kuppel et al., 2018b)) and soil water availability at each layer. Note that, when multiple vegetation types occur in one grid cell, each type is calculated separately and the overall fluxes are summed weighted by their areal proportions.

Water balance is conceptualized using linear bucket-type approaches (**Figure 3a**). Precipitation is firstly intercepted by canopy storage. Throughfall (upon exceeding the maximum canopy storage) and snowmelt (due to any extra energy input into snowpack after reaching the melting temperature) enter into the temporary surface ponding storage. Surface infiltration to the first soil layer is calculated using the Green-Ampt method (Mein and Larson, 1973), and further percolation into deeper layers once the upper layers reached field capacity is approximated kinematically. Vertical percolation from the third soil layer into a deeper groundwater storage was added in Yang et al. (2021) to incorporate deeper groundwater dynamics and their contributions to runoff generation. Lateral exchanges are enabled for free-flowing water storages, i.e., the surface ponding water (as surface overland flow), the third-layer gravitational soil water after exceeding soil field capacity (as subsurface groundwater flow) and the deeper groundwater storage (as deeper baseflow). The subsurface water movement to the downslope cell is calculated using 1-D kinematic wave approaches, which consider effective hydraulic conductivity, slope gradient and available water storage. Due to such terrestrial lateral inputs, re-infiltration and up-ward return flow may occur and are included in the EcH₂O-iso model. For grid cells connected to channels, additional stream runoff generation is considered. Surface ponded water is partitioned into overland flow to the channel and the down-slope cell; the two subsurface runoff components are calculated using an exponential decay function, considering effective hydraulic conductivity, available water storage and a seepage controlling parameter. Channel routing is calculated using a nonlinear kinematic wave model with a parameter of scaled Manning's roughness coefficient.

Modules of vegetation growth dynamic and isotopic tracer tracking are also available in EcH₂O-iso. However, as being out of the scope of the model development and initial coupling tests, the two modules were deactivated in this study.

3.2 Testing model 2: the hydrological mHM model

The mesoscale Hydrological Model mHM (Samaniego et al., 2010) is a fully distributed, HBV-type model (**Figure 3b**). The aboveground compartments are conceptualised through three linear reservoirs (canopy storage, snowpack and impervious surface storage), and fluxes of throughfall and snowmelt are calculated based on a simple threshold behaviour. The effective precipitation (the sum of snowmelt and throughfall) is partitioned into impervious surfaces where a direct runoff component can be generated and pervious surfaces that allow further infiltration into soils. Evapotranspiration is calculated as fulfilling the potential evapotranspiration demand (as model input data) and sequentially taken from the canopy level and soil layers (according to available soil water storage and root fraction at each layer). Water flux percolation from the lowest soil layer enters into the conceptual unsaturated water storage, from which fast interflow (after exceeding a storage threshold) and permanent slow interflow are generated. The conceptual saturated storage receives percolation from the unsaturated storage and generates the baseflow component of runoff. Note that the passive storage was added by Yang et al. (2018), representing



N retention in the deeper groundwater system. All of the four runoff components (direct runoff, fast interflow, slow interflow and baseflow) are summed as the terrestrial total runoff, which enters into channels for stream routing using a linear routing method (e.g., the Muskingum routing method).

One of the key advantages of the mHM implementation is its multi-scale flexible structure and regionalization technique (Samaniego et al., 2010; Kumar et al., 2013). For example, the spatial resolution for channel routing can be separately defined by the users, and terrestrial exports at the modelling resolution will be automatically aggregated.

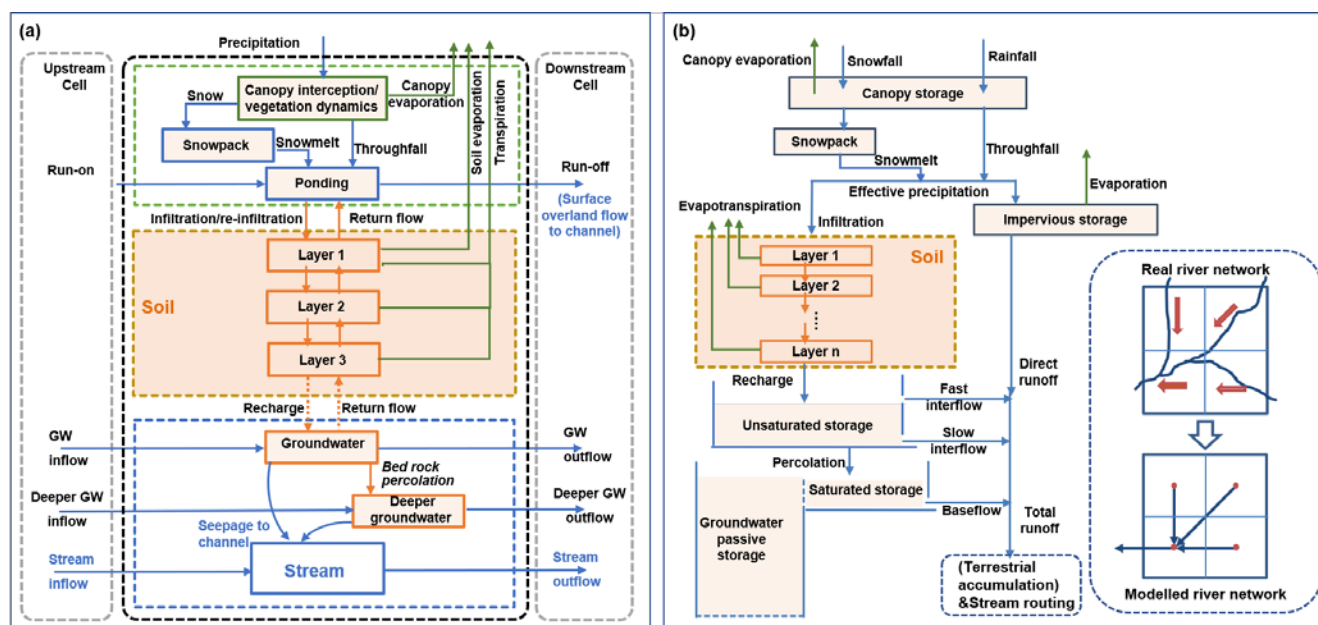


Figure 3. Hydrological structures of the Ech2O-iso model (a) and the mHM model (b). For Ech2O-iso, the seepage to channel and stream routing processes are only considered for channel-connected grid cells; For mHM, if the stream routing resolution is coarser than that of terrestrial modelling, aggregation of terrestrial exports is considered.

3.3 Testing catchment and setups of the two coupled modelling

The HiWaQ-N module was tested in the Silberhütte catchment (99 km², mean elevation 441 m above sea level), located in the lower range of the Harz Mountains, central Germany (Figure 4). The Silberhütte catchment is the headwater of the Selke catchment, as part of Bode observatories of the Terrestrial Environmental Observatories - TERENO project (Wollschläger et al., 2016). The Silberhütte catchment is dominated by forests (consisting of 44.3% coniferous, 12.8% deciduous, and 4.7% mixed forests) and agricultural lands (18.5% arable and 16.1% pastures), with additional 3.4% urban areas (Figure 4b). Major crops cultivated in the arable lands are winter wheat and winter rapeseed, with fertilizer application rates of 158 and 182 kg N ha⁻¹yr⁻¹, respectively (Yang et al., 2022a). The soil and geological properties are uniformly dominated by cambisols and shallow schist/claystone, respectively (Yang et al., 2018; Wollschläger et al., 2016). The flow regime is relatively flashy during winter high-flow periods (Dupas et al., 2017). Further, extensive bedrock fractures result in large deeper groundwater



dynamics, contributing significantly to stream runoff generation especially during summer low-flow periods (Jiang et al., 2014; Yang et al., 2018).

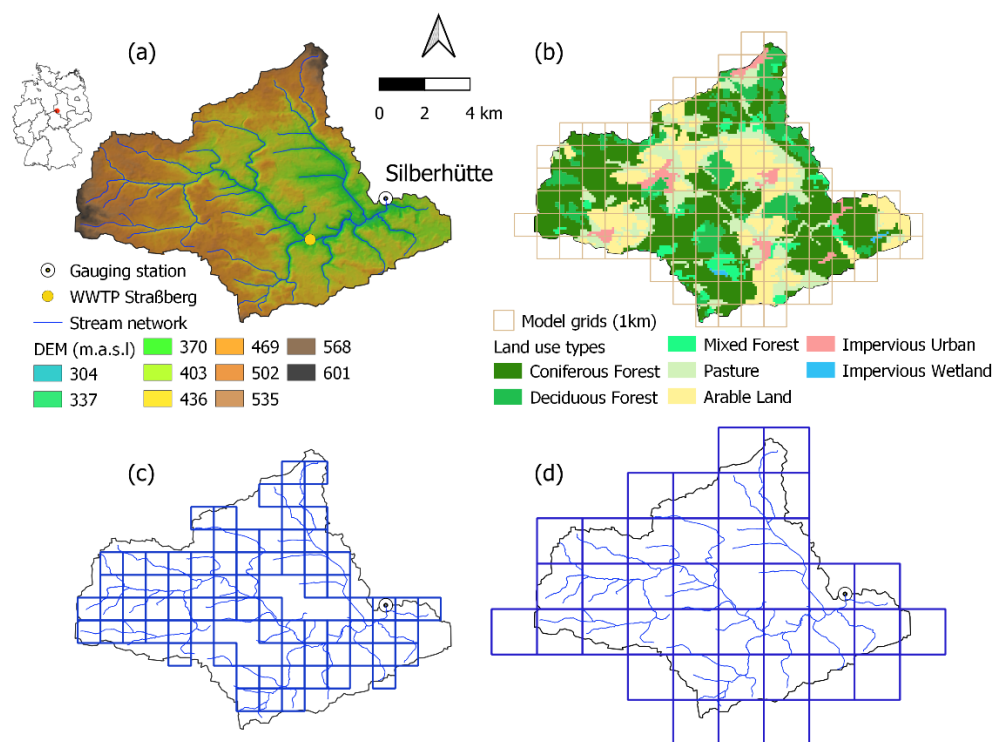


Figure 4. The Silberhütte catchment (99 km²) located in the lower Harz Mountain range, central Germany. (a) Digital elevation model – DEM (30 m, source: ASTER Global Digital Elevation Model), stream network (source: the water authority LHW), and the outlet gauging station Silberhütte; (b) land cover types. Both Ech2O-iso and mHM are set-up in the catchment with 1km² terrestrial modeling resolution (in (b)), while for stream routing, the former calculates only within the mask of real channel network (c) and the latter considers in-stream processes for each grid cell of 2 km² routing resolution (d).

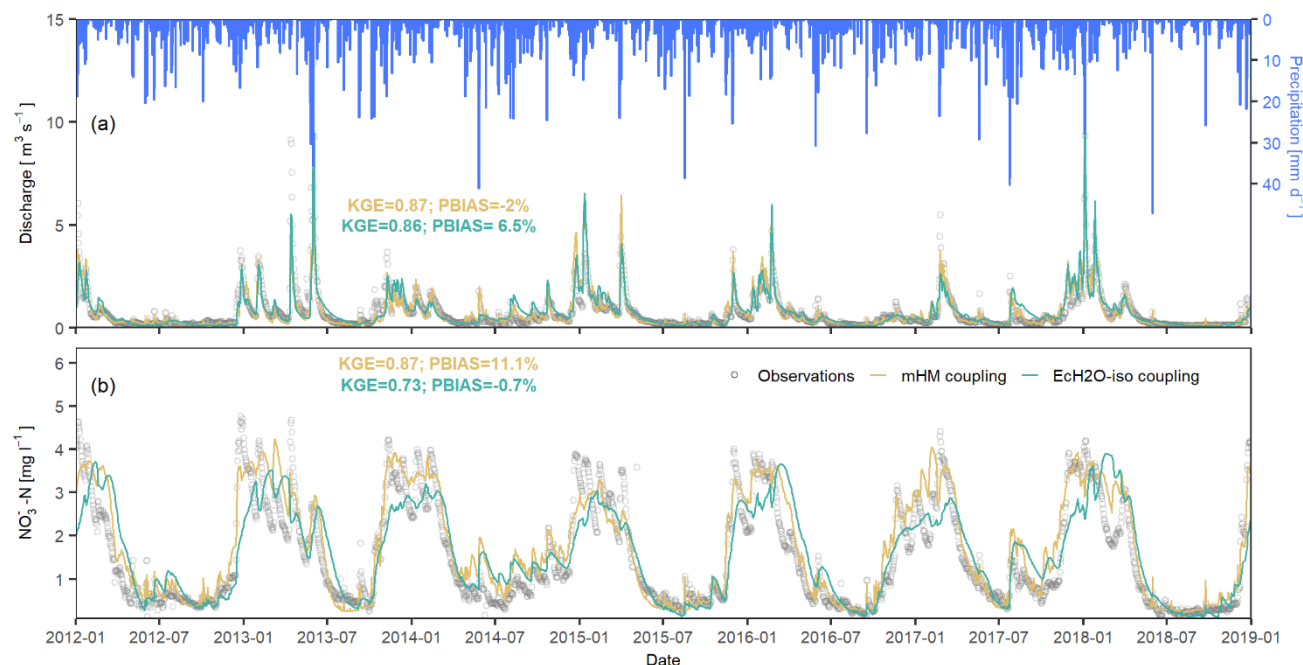
Daily climate forcing data over 2010-2018 were collected from the German Weather Service (DWD, including 51 precipitation stations and 15 climate stations for all meteorological elements). Daily discharge and $\text{NO}_3^- - \text{N}$ concentration observations over 2010-2018 at the outlet gauging station Silberhütte were collected from the water authority LHW (State Agency for Flood Protection and Water Management of Saxony-Anhalt) and the high-frequency monitoring of TERENO project from Helmholtz Centre for Environmental Research - UFZ. Catchment-wide annual precipitation is 806 ± 62 mm, with higher values in the high-elevation boundary areas than in the leeward-positioned central areas. Annually mean temperature is 8.1 °C, ranging from -4.3 to 19.6 °C (5% and 95% quantiles over 2010-2018). Annual runoff depth is ca. 227.7 mm, of which ca. 74.4% is contributed during the wet winter-spring seasons. $\text{NO}_3^- - \text{N}$ concentrations exhibit a similar seasonal pattern (> 4.0 and < 0.5 mg l^{-1} during high- and low-flow periods, respectively), with the yearly mean of 1.59 mg l^{-1} .



EcH₂O-iso and mHM were both setup for daily simulations during 2010-2018 (with the first two years used as a spin-up
 320 period), with the same spatial modelling resolution of 1×1 km (**Figure 4b**). Gridded climatic inputs and catchment
 characteristics (topographic drainage, landuse, soil properties, etc.) were also identically prepared for both model setups.
 Importantly, to test the flexibility of the HiWaQ tool, the two models were set up with different channel configurations, where
 in-stream routing and N processes of the EcH₂O-iso based modelling were considered only within the channel mask of the real
 river network (**Figure 4c**), while for the mHM based modelling they were simulated with a spatial resolution of 2×2 km
 325 (**Figure 4d**). Note that process descriptions of in-stream gross assimilation and re-mineralization by Yang et al. (2019a) were
 chosen in this study (**Table 1**). For the initial testing purpose of this study, the whole period data were used for model
 calibration and the calibrations were conducted in a step-wise manner: (1) flow simulations were firstly calibrated following
 our previous work in Yang et al. (2022b) for EcH₂O-iso and Yang et al. (2018) for mHM; then (2) N module parameters (listed
 in **Table 1**) were calibrated exclusively against $NO_3^- - N$ concentration observations in this study using the Dynamically
 330 Dimensioned Search method (Tolson and Shoemaker, 2007). More details of respective model calibration methods and
 schemes were provided in **Supplementary Text S1**.

3.4 Results of catchment N dynamics and comparisons between the two coupled modelling

Discharge simulations of both EcH₂O-iso and mHM reproduced the observations at station Silberhütte well (**Figure 5a**), in
 terms of seasonal patterns (winter-spring high flows and summer-autumn low flows) and inter-annual variability (the peak
 335 flows differed largely between years under various weather conditions). Discharge performance metrics of both models were
 also almost identical, with KGEs above 0.86 and PBIAS within $\pm 10\%$. Although summer flood events are generally subtle
 compared to overall flow dynamics, the two model simulations showed relatively larger deviations during these periods. The
 mHM simulations always responded rapidly to summer rainfall events, whereas the EcH₂O-iso simulations exhibited smooth
 responses and relatively long-tailed recessions (e.g., the event during 24th July – 29th August 2017).
 340 For $NO_3^- - N$ modelling based on the new HiWaQ-N model, the two coupled model simulations also performed similarly well
 as compared to the daily $NO_3^- - N$ concentration observations (KGE was better, while PBIAS was worse, for the mHM
 coupling than the EcH₂O-iso coupling; **Figure 5b**). Both coupled models well mimicked the high $NO_3^- - N$ concentrations
 during high-flow seasons (during which both simulated fluctuation patterns (though to a lesser extend compared to the
 observations) and reproduced the inter-annual variations consistently. None of the two simulated time series outperformed the
 345 other systematically, and their deviations were not consistent during the whole simulation period. Notably, compared to the
 mHM coupling, the EcH₂O-iso coupling simulations exhibited smoother dynamics of $NO_3^- - N$ concentration during summer
 periods and considerably overestimates during falling limbs of high-concentration events. These deviations were likely in
 accordance with the smoother flow responses to summer events and the longer tailed flood recession patterns.



350 **Figure 5. Discharge (a) and $\text{NO}_3^- - \text{N}$ concentration (b) performances of the coupled modelling with EcH₂O-iso and mHM. KGE-Kling-Gupta Efficiency, ranging from $-\infty$ to 1 (the perfect fitting); PBIAS- percentage bias.**

The two grid-based, coupled modelling approaches similarly simulated the high spatial heterogeneities of major terrestrial N balancing components (**Fig. 6**) and soil stock (**Fig. S1**). N supplies from external applications (**Fig. 6a, e and h**) were identical as defined exclusively by the HiWaQ-N model; supplies from internal remineralization (**Fig. 6b, f and i**) were also almost identical, primary due to (1) that the initial conditions of soil organic N were identically specified in HiWaQ-N and (2) that the $\text{NO}_3^- - \text{N}$ dynamics are normally not very sensitive to the mineralization rate parameter (Yang et al., 2019b). However, N uptake by plants/crops (**Fig. 6c and g**) and removal via denitrification (**Fig. 6d and h**) exhibited slight but important differences between the two couplings (e.g., more uptake for the EcH₂O-iso coupling whereas more denitrification for the mHM coupling among the 17 grid cells with arable area proportion ≥ 0.50 ; **Fig. 6j and k**). Moreover, the uptake and denitrification in the arable lands seem to be compensating each other, leading to similar total removals between the two models (e.g., 138.4 ± 24.5 and $136.1 \pm 22.9 \text{ kg N ha}^{-1} \text{yr}^{-1}$ for the EcH₂O-iso and the mHM couplings, respectively, among the 17 arable-dominant grid cells).

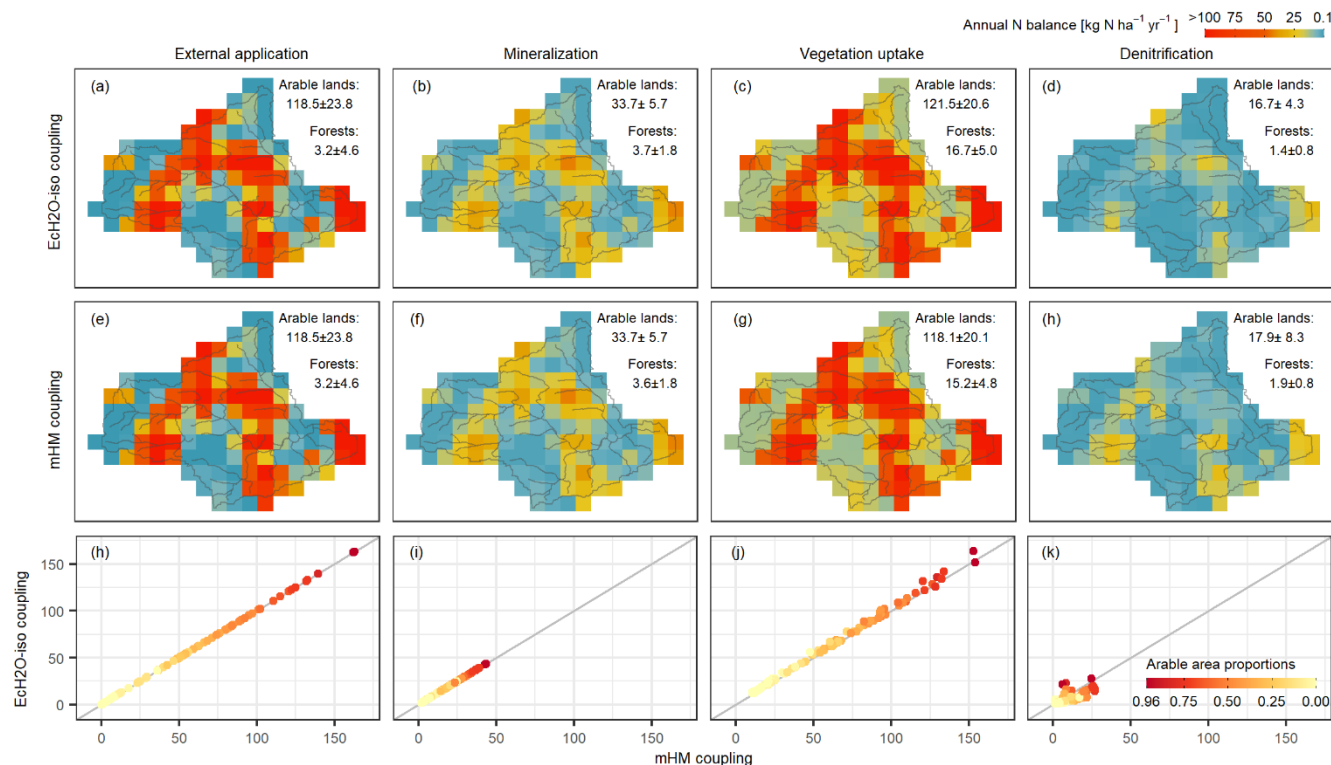


Figure 6. Spatial distributions of catchment N balance simulated based on the HiWaQ coupled with EcH₂O-iso (a-d) and mHM (e-h). Columns from left to right represent external equivalent N application (fertilizer and manure), mineralization from soil N organic stock, annual vegetation uptake and denitrification removal. Mean \pm standard deviation values are presented separately for arable- and forest-dominant grids, defined as area proportion ≥ 0.50 ($n=17$) and > 0.75 ($n=56$), respectively. The subplots h-k with the 1:1 line directly compare the simulated values in each grid cell (both axes are with unit of $\text{kg N ha}^{-1}\text{yr}^{-1}$, and the colour code indicates area proportion of arable lands of each grid cell).

In addition to the well represented spatial variability and the self-compensation of N balancing in the high N level agricultural lands, the two couplings also consistently simulated the temporal variability of catchment-wide $\text{NO}_3^- - \text{N}$ dynamics (Figs. 7 and S2). The overall catchment soil $\text{NO}_3^- - \text{N}$ stock (Fig. 7a) varied substantially during the major growing seasons as jointly impacted by vegetation uptake and the timing of fertilizer inputs (Fig. S2a and c) and reached minimum levels in July-August as the end of the major growing season; then the stock was considerably supplied by the mineralization process throughout the late summer and autumn seasons (Fig. S2b), with certain decreases during the high flow and $\text{NO}_3^- - \text{N}$ exporting periods (Fig. 7b), before the start of the next seasonal cycling. Moreover, both model simulations consistently demonstrated the strong seasonal patterns of network-scale in-stream $\text{NO}_3^- - \text{N}$ retention (including both in-stream denitrification and net assimilatory uptake) and their inter-annual variations (Fig. 7c). The retention amount increased from the beginning of spring, while it generally started to decrease already during early summer when stream $\text{NO}_3^- - \text{N}$ loading dramatically reduced to, e.g., $< 3 \times 10^3$ kg per month (Fig. 7b). This has associated with dramatic increases in retention efficiencies (percentages of total retention amount to total terrestrial export), which remained high throughout the low-loading seasons (Fig. 7c). The retention



during later summer and autumn varied significantly between years, exhibiting much higher retention amount while lower efficiencies in years with higher summer $\text{NO}_3^- - \text{N}$ loading (e.g., in 2014 and 2017). In accordance with the higher terrestrial exports during recession and summer periods (Fig. 7b), the retention of the EcH₂O-iso coupling showed relatively higher retention amount than that of the mHM coupling, while their retention efficiencies were very similar (with even higher efficiencies for the mHM coupling during the relatively high loading summers of 2014 and 2017).

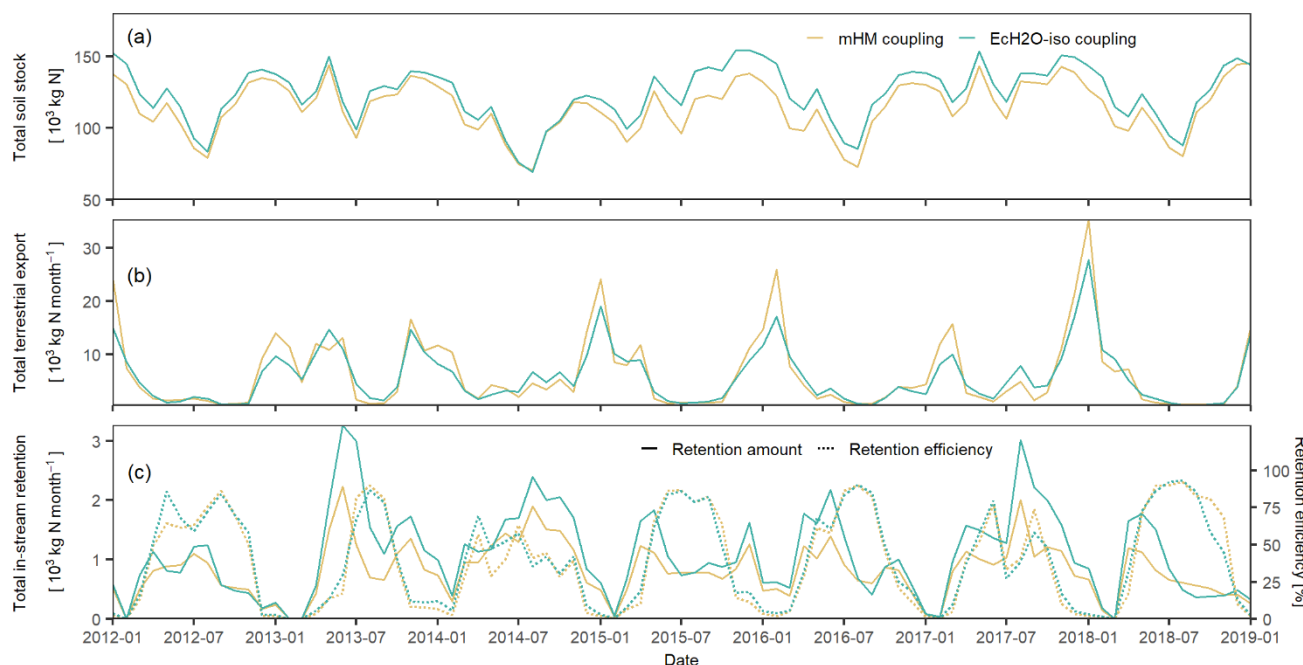


Figure 7. Comparisons of the monthly $\text{NO}_3^- - \text{N}$ amounts of (a) soil stock, (b) terrestrial export and (c) in-stream retention and efficiency simulated by the EcH₂O-iso coupling and the mHM coupling. The retention efficiency was calculated as the percentages of total in-stream retention amount to total terrestrial export.

4 Discussion and outlook

4.1 Insights into catchment N dynamics using different hydrological modelling structures

With equally well simulated discharge by EcH₂O-iso and mHM, the coupled HiWaQ-N simulations successfully and consistently reproduced the temporal dynamics of $\text{NO}_3^- - \text{N}$ concentration observed at the Silberhütte outlet (Fig. 5b), including the clear seasonal patterns and inter-annual variability (e.g., the high values during the extraordinary flooding events in late spring of 2013 and the prolonged low values during extreme droughts in summer-autumn 2018). The temporal patterns of discharge and $\text{NO}_3^- - \text{N}$ concentration were well synchronised (i.e., higher discharge associated with higher concentrations), exhibiting a more chemodynamic $\text{NO}_3^- - \text{N}$ export regime of the catchment. This primarily results from the flashy hydro-climatic regime and shallow bedrock condition that jointly hinder long-term soil N accumulation and its further downward leaching to the regional groundwater system, even for the agricultural areas with high anthropogenic inputs (Dupas



et al., 2017; Yang et al., 2022a). Further, both grid-based modeling consistently reflected the high spatial heterogeneity of catchment N balancing and soil stock in this mixed forest-agricultural catchment. Agricultural activities have elevated soil N levels nearly ten times compared to that of forest soils (**Fig. S1**); this has likely further stimulated more active N transformations like the soil mineralization and denitrification processes (**Fig. 6**). The simulated denitrification amount and its larger variations between agricultural and forest soils fit well with literature ranges, though catchment-scale assessments are still relatively rare (Oehler et al., 2009; Hofstra and Bouwman, 2005; Barton et al., 1999). In-stream $\text{NO}_3^- - \text{N}$ retention is also believed to play essential roles on catchment water quality and overall nitrate export to receiving water bodies (Mulholland, 2004; Helton et al., 2011; Yang et al., 2019a). The simulated network-scale retention showed strong seasonal patterns, which also differed in terms of the retention amount and the retention efficiency (**Fig. 7c**). This could primarily result from combined impacts of multiple stream environmental factors: increasing temperature and radiation conditions from the beginning of spring likely result the dramatic increases of in-stream retention amount; however, from late spring/early summer, the in-stream processes were largely constrained by the dramatically reduced stream $\text{NO}_3^- - \text{N}$ levels (indicated by the high retention efficiencies) and stream light availability (shaded by the closed canopy of riparian deciduous vegetation (Yang et al., 2019a)).

In addition to the general consistency in revealing catchment-wide N dynamics, simulations of the EcH₂O-iso coupling and the mHM coupling exhibited subtle but insightful differences that are plausibly derived from the contrasting hydrological model structures. Although process descriptions and catchment treatments are more physically grounded in EcH₂O-iso than in mHM (**Fig. 3** and **Table S1**), the EcH₂O-iso flow simulations during small summer events exhibited smoother responses and longer tailed recessions and the performance was relatively poor, compared to that of the conceptual mHM (**Fig. 5a**). This agrees that more complex process-based hydrological structures do not necessarily perform better than simpler ones at larger scale catchments (Tetzlaff et al., 2008; Orth et al., 2015). Such modelling differences were obviously leveraged in the HiWaQ $\text{NO}_3^- - \text{N}$ simulations, i.e., the simulated stream $\text{NO}_3^- - \text{N}$ concentrations exhibited higher degrees of divergence between the two couplings (**Fig. 5b**). This, in turn, implied that catchment water quality data could also be sensitively indicative for hydrological simulations and that its information content could be complementary to that of conventional hydrometric data (with the fundamental reasoning of solute particle movement at velocity vs pressure wave propagation at celerity (Hrachowitz et al., 2016)).

Moreover, vegetation N uptake and denitrification removal likely self-compensated, resulting in similar levels of total output from the two couplings, especially in the high-N agricultural areas (**Figs. 6**). The EcH₂O-iso coupling estimated higher vegetation N uptake, plausibly due to the enabled lateral flow exchanges between grid cells in EcH₂O-iso (**Fig. 3a**), which can increase soil water availability, thereby relaxing soil water constraints of vegetation N uptake. However, this likely reduced nitrate availability for soil denitrification, although higher soil water condition is favourable for this anaerobic process (Yang et al., 2019b; Soana et al., 2022). Further tackling model structural uncertainty of such complex, integrated catchment models remains challenging (Beven, 2007), which ultimately call for advancing interdisciplinary integrations of data and theories (Li et al., 2021; Yang et al., 2022a). Similar to the multi-model philosophy in hydrological modelling (Duan et al., 2007; Clark et al., 2008), cross-comparisons of catchment nutrient simulations using contrasting hydrological models (e.g., using the



435 developed HiWaQ tool) might be a more practical alternative in guiding science-based catchment water quantity-quality management.

4.2 Flexibility and strengths of HiWaQ

HiWaQ aims to facilitate convenient catchment water quality assessments that take advantages of advanced hydrological modelling, therefore, its flexibility of incorporating with various hydrological model structures is one of the key priorities
 440 throughout the development. Particularly, it is realised through:

- The implementation of the unified coupling interface that allows specifying spatial discretization schemes (semi-distributed vs grid-based) and drainage configurations (terrestrial hydrological connectivity and stream channel networks). Catchment configurations for the semi-distributed type are relatively simple, where vertical heterogeneity and lateral connectivity of water movement are mainly considered at the HRU and the sub-catchment levels,
 445 respectively. However, it is more variable and flexible for the grid-based type. As tested by the EcH₂O-iso coupling, HiWaQ is suitable for coupling with more complex, process-based ecohydrological models, which e.g., enables lateral subsurface flux exchanges between grid cells and independent terrestrial-channel exchanges according to the real river network. As tested by the mHM coupling, HiWaQ is also capable of handling multi-scale hydrological modelling, which involves internal spatial aggregations of state variables and fluxes.
- The inclusion of a comprehensive consideration of various hydrological processes (**Fig. 1b**). HiWaQ facilitates flexible specification of hydrological processes and related variables of fluxes and storages, in accordance with the coupled hydrological model structure. This has been well validated by the successful couplings with EcH₂O-iso and mHM, given their substantial structural differences (**Fig. 3**). Moreover, the consistency between the specified processes and related variables is ensured through sequences of quality checks implemented in the HiWaQ codes,
 455 accompanied with detailed documentations and debugging messages (Yang et al., 2022b).
- The design of the generalised structure of storage-flux interactions for both physical and conceptual storages (**Fig. 1c**). Among others, the setting differentiation for the “*up_in*” flux of conceptual storages ingeniously generalises the differences in hydrological conceptualisations. For example, the “groundwater storage” in EcH₂O-iso (**Fig. 4a**) is not an independent storage but represents the gravitational part of the soil water storage at the third soil layer; therefore,
 460 its “*up_in*” flux variable should be set as “none” in HiWaQ, indicating that its concentration is directly replaced with that of its source storage. In contrast, the “unsaturated storage” in mHM (**Fig. 4b**) represents an independent conceptual storage that receives soil water recharge (the flux assigned to the “*up_in*” variable) and supplies interflow generation and percolation to deeper groundwater; therefore, HiWaQ treats it as a normal storage, of which $NO_3^- - N$ concentration is calculation based on the full mixing assumption.

465 To our knowledge, HiWaQ is one of the first catchment water quality simulation tools that emphasise such coupling capability to multiple hydrological model structures. As inherited from previous mHM-Nitrate implementations (Yang et al., 2018; Yang and Rode, 2020), impacts of anthropogenic activities on catchment water quality are also comprehensively considered,



including both diffuse sources (agricultural management practices in terms of fertilizer application and crop rotation) and point sources (time-varying inputs at specific locations). Moreover, each of the introduced parameters (e.g., **Table 1** for nitrate-related biogeochemical reaction rates) can be independently specified as either land-use or soil type dependent and further grouped into a smaller number of categories, ensuring a more flexible and parsimonious parameterisation scheme for the water quality module.

With the above generalisation concerns of hydrological structures and advanced water quality modelling implementations, HiWaQ offers new potential for simultaneous, robust catchment water quantity and quality assessments. Cross-comparison and integration of multiple model structures are commonly conducted in hydrological modelling community, as a learning process of handling model structural errors (Beven, 2007; Clark et al., 2008) and of improving understanding of the complex catchment system (Clark et al., 2011); building on this, HiWaQ provides a unified framework that represents a step forward in extending such multi-model strategies to catchment water quality modelling. Water quality-related boundary conditions and anthropogenic activities are identically set in HiWaQ, such that differences in simulated water quality status can be better attributed to different hydrological structures. This is particularly essential for the coupled environmental modelling which usually exhibits higher degrees of complexity and equifinality problems (Li et al., 2021; Beven and Freer, 2001).

HiWaQ does not implement any flow simulation modules, but exclusively relying on external hydrological modelling. This avoids pre-selections among tremendous available hydrological structures, which might differ throughout the model building, e.g., the five steps summarised by Gupta et al. (2012): conceptual physical structure, conceptual process structure, spatial variability structure, equation structure, and computational structure. Meanwhile, such a loose coupling strategy (i.e., exchanges of hydrological fluxes and state variables via the common NetCDF format) relaxes complex technical integration between various modelling platforms and programming languages. Overall, HiWaQ can make most use of existing (eco-)hydrological modelling that embeds thoughtful modelling thinking and localised perceptual knowledge, and can better leverage these advancements in the simultaneous catchment water quantity-quality assessment.

4.3 Limitations and Outlook

As an initial development, we also noted that there are also several aspects of limitations in the current HiWaQ implementation:

- It is restricted to the bucket-type modelling system that is solved by one-dimensional ODEs, and therefore, it is not compatible with hydrological models containing any 2-D/3-D components.
- The full-mixing assumption is applied to all storages, and the storage volume differentiation between hydrologically dynamic and passive parts is only possible for the deep groundwater storage (usually generating low and constant baseflow, but its solute signals could be largely attenuated by regional groundwater systems). Further development can be directed to enable the dynamic- and passive-volume differentiation option for each subsurface storage (e.g., in Birkel et al. (2011) and Wade et al. (2002)) and thereafter, to implement the option for the partial mixing between the differentiated volumes (e.g., following Hrachowitz et al. (2013)).



- 500
- Options of hydrological compartments and processes can be further extended. For example, tile drainage process is not considered yet given that detailed tile drain information is usually absent at catchment scale, while it might substantially alter hydrological and water quality dynamics in agricultural catchments and should be considered (e.g., as shown in Li et al. (2010)).
 - As a drawback of the loose coupling, per time-step interaction with external hydrological models is not possible.
- 505
- This may involve heavy I/O processing, especially for larger-scale coupling and for larger-number iterative model analysis. Several solutions are possible to work around this. Associated with the open-access model codes, we provided a python script that helps arranging parallel running using array jobs, while the implementation of MPI-based parallel computing is underway.

Nevertheless, the development of HiWaQ-N and its coupling tests with the contrasting EcH₂O-iso and mHM models, demonstrated that the current HiWaQ tool satisfies its general aims in terms of providing robust estimates of catchment N dynamics and facilitating insightful cross-comparisons between couplings with different hydrological structures. Further exploiting the coupled catchment modelling, e.g., better integrating nitrate dynamics with the EcH₂O-iso simulations of vegetation dynamics and water ages, can potentially inspire advanced insights into the complex environmental systems. Moreover, it is also highly promising to further extend the platform to other nutrients and pollutants (e.g., phosphorus, carbon, and their intrinsic stoichiometric relations), to further couple the platform with various, contrasting hydrological models and to apply the coupled modelling to catchments under different climatic and anthropogenic conditions.

515

By facilitating such a generalised, flexible coupling, we believe that this framework can bring together catchment hydrologists and environmental scientists in a technically easier way; In turn, with tremendous expertise of the open-source earth system model community, we hope that interested researchers and model developers can be involved in and contribute their knowledge and skills to the further development, which is oriented to be scientifically insightful for catchment modelling and practically useful for catchment management.

520

Code availability. The HiWaQ source code and documentation can be found at https://github.com/XYang-EcoHydroWQ/HiWaQ_v1.0 (last access: 23th September 2022) and an archived version at <https://doi.org/10.5281/zenodo.7107394> (Yang et al., 2022b). The EcH₂O-iso model source code can be found at [https://github.com/XYang-EcoHydroWQ/EcH₂O-iso_largescale](https://github.com/XYang-EcoHydroWQ/EcH2O-iso_largescale), and mHM at <https://git.ufz.de/mhm/mhm> (this work used the version v5.5).

525

Data availability. The testing data in the Silberhütte catchment and coupling configurations related to this work are available at <https://doi.org/10.48758/ufz.12943> (Yang, 2022).

530

Supplement. The supplement related to this article is available



Author contributions. XY coded the HiWaQ framework and conducted the coupling tests in the Silberhütte catchment. DT, CS and DB conceived the initial ideas, and all co-authors were involved in the design of the modelling framework and the interpretation of results. XY prepared the manuscript with significant contributions from all co-authors.

Competing interests. The authors declare that they have no conflict of interest.

Acknowledgement. This work was supported by the Modular Observation Solutions for Earth Systems – MOSES project and the Terrestrial Environmental Observatories – TERENO project of the Helmholtz Association, Germany. Funding was received for Doerthe Tetzlaff through the Einstein Research Unit “Climate and Water under Change” from the Einstein Foundation Berlin and Berlin University Alliance. Contributions by Chris Soulsby were supported by the Leverhulme Trust through the ISO-LAND project (RPG 2018 375). We thank Michael Rode for the general discussion of water quality model development. The authors also thank the German Weather Service (DWD), the Federal Institute for Geosciences and Natural Resources (BGR) and the State Agency for Flood Protection and Water Management Saxony-Anhalt (LHW) for the model setup data.

References

- Andersson, L., Rosberg, J., Pers, B. C., Olsson, J., and Arheimer, B.: Estimating Catchment Nutrient Flow with the HBV-NP Model: Sensitivity to Input Data, *Ambio*, 34, 521–532, 2005.
- Arnold, J. G., Srinivasan, R., Muttiah, R. S., and Williams, J. R.: Large area hydrologic modeling and assesment Part I: Model development, *J. Am. Water Resour. Assoc.*, 34, 73–89, <https://doi.org/10.1111/j.1752-1688.1998.tb05961.x>, 1998.
- Barton, L., McLay, C. D. A., Schipper, L. A., and Smith, C. T.: Annual denitrification rates in agricultural and forest soils: a review, *Soil Res.*, 37, 1073–1094, 1999.
- Bergström, S.: The HBV model, in: *Computer Models of Watershed Hydrology*, edited by: Singh, V. P., Water Resour. Publ., Highlands Ranch, CO, 443–476, 1995.
- Beven, K.: Towards integrated environmental models of everywhere: Uncertainty, data and modelling as a learning process, *Hydrol. Earth Syst. Sci.*, 11, 460–467, <https://doi.org/10.5194/hess-11-460-2007>, 2007.
- Beven, K. and Freer, J.: Equifinality, data assimilation, and uncertainty estimation in mechanistic modelling of complex environmental systems using the GLUE methodology, *J. Hydrol.*, 249, 11–29, [https://doi.org/10.1016/S0022-1694\(01\)00421-8](https://doi.org/10.1016/S0022-1694(01)00421-8), 2001.
- Bicknell, B. R., Imhoff, J. C., Kittle, J. L., Donigian, A. S., and Johanson, R. C.: *Hydrological Simulation Program FORTRAN: User’s Manual for Version 11*, U.S. Environmental Protection Agency, Athens, Georgia, 1997.
- Birkel, C., Soulsby, C., and Tetzlaff, D.: Modelling catchment-scale water storage dynamics: reconciling dynamic storage with



- tracer-inferred passive storage, *Hydrol. Process.*, 25, 3924–3936, <https://doi.org/10.1002/hyp.8201>, 2011.
- Brauman, K. A.: Hydrologic ecosystem services: linking ecohydrologic processes to human well-being in water research and watershed management, *WIREs Water*, 2, 345–358, <https://doi.org/10.1002/wat2.1081>, 2015.
- Clark, M. P., Slater, A. G., Rupp, D. E., Woods, R. A., Vrugt, J. A., Gupta, H. V., Wagener, T., and Hay, L. E.: Framework
 570 for Understanding Structural Errors (FUSE): A modular framework to diagnose differences between hydrological models, *Water Resour. Res.*, 44, <https://doi.org/10.1029/2007WR006735>, 2008.
- Clark, M. P., Kavetski, D., and Fenicia, F.: Pursuing the method of multiple working hypotheses for hydrological modeling, *Water Resour. Res.*, 47, <https://doi.org/10.1029/2010WR009827>, 2011.
- Clark, M. P., Bierkens, M. F. P., Samaniego, L., Woods, R. A., Uijlenhoet, R., Bennett, K. E., Pauwels, V. R. N., Cai, X.,
 575 Wood, A. W., and Peters-Lidard, C. D.: The evolution of process-based hydrologic models: historical challenges and the collective quest for physical realism, *Hydrol. Earth Syst. Sci.*, 21, 3427–3440, <https://doi.org/10.5194/hess-21-3427-2017>, 2017a.
- Clark, M. P., Bierkens, M. F. P., Samaniego, L., Woods, R. A., Uijlenhoet, R., Bennett, K. E., Pauwels, V. R. N., Cai, X.,
 580 Wood, A. W., and Peters-Lidard, C. D.: The evolution of process-based hydrologic models: historical challenges and the collective quest for physical realism, *Hydrol. Earth Syst. Sci.*, 21, 3427–3440, <https://doi.org/10.5194/hess-21-3427-2017>, 2017b.
- Duan, Q., Ajami, N. K., Gao, X., and Sorooshian, S.: Multi-model ensemble hydrologic prediction using Bayesian model averaging, *Adv. Water Resour.*, 30, 1371–1386, <https://doi.org/10.1016/j.advwatres.2006.11.014>, 2007.
- Dupas, R., Musolff, A., Jawitz, J. W., Rao, P. S. C., Jäger, C. G., Fleckenstein, J. H., Rode, M., and Borchardt, D.: Carbon and
 585 nutrient export regimes from headwater catchments to downstream reaches, *Biogeosciences*, 14, 4391–4407, <https://doi.org/10.5194/bg-14-4391-2017>, 2017.
- Gupta, H. V., Clark, M. P., Vrugt, J. A., Abramowitz, G., and Ye, M.: Towards a comprehensive assessment of model structural adequacy, *Water Resour. Res.*, 48, <https://doi.org/10.1029/2011WR011044>, 2012.
- Guswa, A. J., Brauman, K. A., Brown, C., Hamel, P., Keeler, B. L., and Sayre, S. S.: Ecosystem services: Challenges and
 590 opportunities for hydrologic modeling to support decision making, *Water Resour. Res.*, 50, 4535–4544, <https://doi.org/10.1002/2014WR015497>, 2014.
- Helton, A. M., Poole, G. C., Meyer, J. L., Wollheim, W. M., Peterson, B. J., Mulholland, P. J., Bernhardt, E. S., Stanford, J. A., Arango, C., Ashkenas, L. R., Cooper, L. W., Dodds, W. K., Gregory, S. V., Hall Jr, R. O., Hamilton, S. K., Johnson, S. L., McDowell, W. H., Potter, J. D., Tank, J. L., Thomas, S. M., Valett, H. M., Webster, J. R., and Zeglin, L.: Thinking outside the
 595 channel: modeling nitrogen cycling in networked river ecosystems, *Front. Ecol. Environ.*, 9, 229–238, <https://doi.org/10.1890/080211>, 2011.
- Hofstra, N. and Bouwman, A. F.: Denitrification in Agricultural Soils: Summarizing Published Data and Estimating Global Annual Rates, *Nutr. Cycl. Agroecosystems*, 72, 267–278, <https://doi.org/10.1007/s10705-005-3109-y>, 2005.
- Hrachowitz, M., Savenije, H., Bogaard, T. A., Tetzlaff, D., and Soulsby, C.: What can flux tracking teach us about water age



- 600 distribution patterns and their temporal dynamics?, *Hydrol. Earth Syst. Sci.*, 17, 533–564, <https://doi.org/10.5194/hess-17-533-2013>, 2013.
- Hrachowitz, M., Benettin, P., van Breukelen, B. M., Fovet, O., Howden, N. J. K., Ruiz, L., van der Velde, Y., and Wade, A. J.: Transit times—the link between hydrology and water quality at the catchment scale, <https://doi.org/10.1002/wat2.1155>, 2016.
- 605 Jarvis, P. G.: The interpretation of the variations in leaf water potential and stomatal conductance found in canopies in the field, *Philos. Trans. R. Soc. London. B, Biol. Sci.*, 273, 593–610, <https://doi.org/10.1098/rstb.1976.0035>, 1976.
- Jawitz, J. W., Desormeaux, A. M., Annable, M. D., Borchardt, D., and Dobberfuhl, D.: Disaggregating Landscape-Scale Nitrogen Attenuation Along Hydrological Flow Paths, *J. Geophys. Res. Biogeosciences*, 125, <https://doi.org/10.1029/2019JG005229>, 2020.
- 610 Jiang, S., Jomaa, S., and Rode, M.: Modelling inorganic nitrogen leaching in nested mesoscale catchments in central Germany, *Ecohydrology*, 7, 1345–1362, <https://doi.org/10.1002/eco.1462>, 2014.
- Keeler, B. L., Polasky, S., Brauman, K. A., Johnson, K. A., Finlay, J. C., O'Neill, A., Kovacs, K., and Dalzell, B.: Linking water quality and well-being for improved assessment and valuation of ecosystem services, *Proc. Natl. Acad. Sci.*, 109, 18619–18624, <https://doi.org/10.1073/pnas.1215991109>, 2012.
- 615 Kroon, F. J., Thorburn, P., Schaffelke, B., and Whitten, S.: Towards protecting the Great Barrier Reef from land-based pollution, *Glob. Chang. Biol.*, 22, 1985–2002, <https://doi.org/10.1111/gcb.13262>, 2016.
- Kumar, R., Samaniego, L., and Attinger, S.: Implications of distributed hydrologic model parameterization on water fluxes at multiple scales and locations, *Water Resour. Res.*, 49, <https://doi.org/10.1029/2012WR012195>, 2013.
- Kuppel, S., Tetzlaff, D., Maneta, M. P., and Soulsby, C.: EcH2O-iso 1.0: water isotopes and age tracking in a process-based, distributed ecohydrological model, *Geosci. Model Dev.*, 11, 3045–3069, <https://doi.org/10.5194/gmd-11-3045-2018>, 2018a.
- 620 Kuppel, S., Tetzlaff, D., Maneta, M. P., and Soulsby, C.: What can we learn from multi-data calibration of a process-based ecohydrological model?, *Environ. Model. Softw.*, 101, 301–316, <https://doi.org/10.1016/j.envsoft.2018.01.001>, 2018b.
- Li, H., Sivapalan, M., Tian, F., and Liu, D.: Water and nutrient balances in a large tile-drained agricultural catchment: a distributed modeling study, *Hydrol. Earth Syst. Sci.*, 14, 2259–2275, <https://doi.org/10.5194/hess-14-2259-2010>, 2010.
- 625 Li, L., Sullivan, P. L., Benettin, P., Cirpka, O. A., Bishop, K., Brantley, S. L., Knapp, J. L. A., van Meerveld, I., Rinaldo, A., Seibert, J., Wen, H., and Kirchner, J. W.: Toward catchment hydro-biogeochemical theories, *Wiley Interdiscip. Rev. Water*, 8, e1495, <https://doi.org/10.1002/wat2.1495>, 2021.
- Lindström, G., Pers, C., Rosberg, J., Strömqvist, J., and Arheimer, B.: Development and testing of the HYPE (Hydrological Predictions for the Environment) water quality model for different spatial scales, *Hydrol. Res.*, 41, 295–319, <https://doi.org/10.2166/nh.2010.007>, 2010.
- 630 Maneta, M. P. and Silverman, N. L.: A Spatially Distributed Model to Simulate Water, Energy, and Vegetation Dynamics Using Information from Regional Climate Models, *Earth Interact.*, 17, 1–44, <https://doi.org/10.1175/2012ei000472.1>, 2013.
- Mein, R. G. and Larson, C. L.: Modeling infiltration during a steady rain, *Water Resour. Res.*, 9, 384–394,



- <https://doi.org/10.1029/WR009i002p00384>, 1973.
- 635 Van Meter, K. J., Van Cappellen, P., and Basu, N. B.: Legacy nitrogen may prevent achievement of water quality goals in the Gulf of Mexico, *Science* (80-.), 360, 427–430, <https://doi.org/10.1126/science.aar4462>, 2018.
- Millennium Ecosystem Assessment: Ecosystems and Human Well-being: General Synthesis, Washington, DC, 2005.
- Mulholland, P. J.: The importance of in-stream uptake for regulating stream concentrations and outputs of N and P from a forested watershed: evidence from long-term chemistry records for Walker Branch Watershed, *Biogeochemistry*, 70, 403–426, <https://doi.org/10.1007/s10533-004-0364-y>, 2004.
- 640 National Academies of Sciences, Engineering, and M.: Thriving on Our Changing Planet: A Decadal Strategy for Earth Observation from Space, National Academies Press, Washington, D.C., <https://doi.org/10.17226/24938>, 2018.
- Norling, M. D., Jackson-Blake, L. A., Calidonio, J.-L. G., and Sample, J. E.: Rapid development of fast and flexible environmental models: the Mobiusframework v1.0, *Geosci. Model Dev.*, 14, 1885–1897, [https://doi.org/10.5194/gmd-14-](https://doi.org/10.5194/gmd-14-1885-2021)
- 645 1885-2021, 2021.
- Oehler, F., Durand, P., Bordenave, P., Saadi, Z., and Salmon-Monviola, J.: Modelling denitrification at the catchment scale, *Sci. Total Environ.*, 407, 1726–1737, <https://doi.org/10.1016/j.scitotenv.2008.10.069>, 2009.
- Oldham, C. E., Farrow, D. E., and Peiffer, S.: A generalized Damköhler number for classifying material processing in hydrological systems, *Hydrol. Earth Syst. Sci.*, 17, 1133–1148, <https://doi.org/10.5194/hess-17-1133-2013>, 2013.
- 650 Orth, R., Staudinger, M., Seneviratne, S. I., Seibert, J., and Zappa, M.: Does model performance improve with complexity? A case study with three hydrological models, *J. Hydrol.*, 523, 147–159, <https://doi.org/10.1016/j.jhydrol.2015.01.044>, 2015.
- Reichert, P., Borchardt, D., Henze, M., Rauch, W., Shanahan, P., Somlyódy, L., and Vanrolleghem, P.: River Water Quality Model no. 1 (RWQM1): II. Biochemical process equations, in: *Water Science and Technology*, 11–30, <https://doi.org/10.2166/wst.2001.0241>, 2001.
- 655 Reusch, T. B. H., Dierking, J., Andersson, H. C., Bonsdorff, E., Carstensen, J., Casini, M., Czajkowski, M., Hasler, B., Hinsby, K., Hyytiäinen, K., Johannesson, K., Jomaa, S., Jormalainen, V., Kuosa, H., Kurland, S., Laikre, L., MacKenzie, B. R., Margonski, P., Melzner, F., Oesterwind, D., Ojaveer, H., Refsgaard, J. C., Sandström, A., Schwarz, G., Tonderski, K., Winder, M., and Zandersen, M.: The Baltic Sea as a time machine for the future coastal ocean, <https://doi.org/10.1126/sciadv.aar8195>, 2018.
- 660 Rockström, J., Steffen, W., Noone, K., Persson, Å., Chapin, F. S., Lambin, E. F., Lenton, T. M., Scheffer, M., Folke, C., Schellnhuber, H. J., Nykvist, B., de Wit, C. A., Hughes, T., van der Leeuw, S., Rodhe, H., Sörlin, S., Snyder, P. K., Costanza, R., Svedin, U., Falkenmark, M., Karlberg, L., Corell, R. W., Fabry, V. J., Hansen, J., Walker, B., Liverman, D., Richardson, K., Crutzen, P., and Foley, J. A.: A safe operating space for humanity, *Nature*, 461, 472–475, <https://doi.org/10.1038/461472a>, 2009.
- 665 Rode, M., Arhonditsis, G., Balin, D., Kebede, T., Krysanova, V., van Griensven, A., and van der Zee, S. E. A. T. M.: New challenges in integrated water quality modelling, *Hydrol. Process.*, 24, 3447–3461, <https://doi.org/10.1002/hyp.7766>, 2010.
- Samaniego, L., Kumar, R., and Attinger, S.: Multiscale parameter regionalization of a grid-based hydrologic model at the



- mesoscale, *Water Resour. Res.*, 46, <https://doi.org/10.1029/2008WR007327>, 2010.
- Shanahan, P., Borchardt, D., Henze, M., Rauch, W., Reichert, P., Somlyódy, L., and Vanrolleghem, P.: River Water Quality
 670 Model no. 1 (RWQM1): I. Modelling approach, in: *Water Science and Technology*, 1–9,
<https://doi.org/10.2166/wst.2001.0238>, 2001.
- Smith, A., Tetzlaff, D., Kleine, L., Maneta, M., and Soulsby, C.: Quantifying the effects of land use and model scale on water
 partitioning and water ages using tracer-aided ecohydrological models, *Hydrol. Earth Syst. Sci.*, 25, 2239–2259,
<https://doi.org/10.5194/hess-25-2239-2021>, 2021.
- 675 Soana, E., Vincenzi, F., Colombani, N., Mastrocicco, M., Fano, E. A., and Castaldelli, G.: Soil Denitrification, the Missing
 Piece in the Puzzle of Nitrogen Budget in Lowland Agricultural Basins, *Ecosystems*, 25, 633–647,
<https://doi.org/10.1007/s10021-021-00676-y>, 2022.
- Soulsby, C., Gibbins, C., Wade, A. ., Smart, R., and Helliwell, R.: Water quality in the Scottish uplands: a hydrological
 perspective on catchment hydrochemistry, *Sci. Total Environ.*, 294, 73–94, [https://doi.org/10.1016/S0048-9697\(02\)00057-8](https://doi.org/10.1016/S0048-9697(02)00057-8),
 680 2002.
- Stanford, G., Dzienia, S., and Vander Pol, R. A.: Effect of Temperature on Denitrification Rate in Soils, *Soil Sci. Soc. Am. J.*,
 39, 867–870, <https://doi.org/10.2136/sssaj1975.03615995003900050024x>, 1975.
- Tetzlaff, D., McDonnell, J. J., Uhlenbrook, S., McGuire, K. J., Bogaart, P. W., Naef, F., Baird, A. J., Dunn, S. M., and Soulsby,
 C.: Conceptualizing catchment processes: simply too complex?, *Hydrol. Process.*, 22, 1727–1730,
 685 <https://doi.org/10.1002/hyp.7069>, 2008.
- Tolson, B. A. and Shoemaker, C. A.: Dynamically dimensioned search algorithm for computationally efficient watershed
 model calibration, *Water Resour. Res.*, 43, <https://doi.org/10.1029/2005WR004723>, 2007.
- Tscheikner-Gratl, F., Bellos, V., Schellart, A., Moreno-Rodenas, A., Muthusamy, M., Langeveld, J., Clemens, F., Benedetti,
 L., Rico-Ramirez, M. A., de Carvalho, R. F., Breuer, L., Shucksmith, J., Heuvelink, G. B. M., and Tait, S.: Recent insights on
 690 uncertainties present in integrated catchment water quality modelling, <https://doi.org/10.1016/j.watres.2018.11.079>, 2019.
- Unidata: Network Common Data Form -NetCDF - Fortran, UCAR/Unidata [software], <https://doi.org/10.5065/D6H70CW6>,
 2022.
- Wade, A. J., Durand, P., Beaujouan, V., Wessel, W. W., Raat, K. J., Whitehead, P. G., Butterfield, D., Rankinen, K., and
 Lepisto, A.: A nitrogen model for European catchments: INCA, new model structure and equations, *Hydrol. Earth Syst. Sci.*,
 695 6, 559–582, <https://doi.org/10.5194/hess-6-559-2002>, 2002.
- Wellen, C., Kamran-Disfani, A.-R., and Arhonditsis, G. B.: Evaluation of the Current State of Distributed Watershed Nutrient
 Water Quality Modeling, *Environ. Sci. Technol.*, 49, 3278–3290, <https://doi.org/10.1021/es5049557>, 2015.
- Wollschläger, U., Attinger, S., Borchardt, D., Brauns, M., Cuntz, M., Dietrich, P., Fleckenstein, J. H., Friesen, K., Friesen, J.,
 Harpke, A., Hildebrandt, A., Jäkel, G., Kamjunke, N., Knöller, K., Kögler, S., Kolditz, O., Krieg, R., Kumar, R., Lausch, A.,
 700 Liess, M., Marx, A., Merz, R., Mueller, C., Musolff, A., Norf, H., Oswald, S. E., Rebmann, C., Reinstorf, F., Rode, M., Rink,
 K., Rinke, K., Samaniego, L., Vieweg, M., Vogel, H.-J., Weitere, M., Werban, U., Zink, M., and Zacharias, S.: The Bode



- hydrological observatory: a platform for integrated, interdisciplinary hydro-ecological research within the TERENO Harz/Central German Lowland Observatory, *Environ. Earth Sci.*, 76, 29, <https://doi.org/10.1007/s12665-016-6327-5>, 2016.
- Yang, X.: HiWaQ coupling tests with EcH2O-iso and mHM in the Silberhütte catchment [data set], Helmholtz Centre for Environmental Research, <https://doi.org/10.48758/ufz.12943>, 2022.
- Yang, X. and Rode, M.: A Fully Distributed Catchment Nitrate Model - mHM-Nitrate v2.0, Zenodo [code], <https://doi.org/10.5281/zenodo.3891629>, 2020.
- Yang, X., Jomaa, S., Zink, M., Fleckenstein, J. H., Borchardt, D., and Rode, M.: A new fully distributed model of nitrate transport and removal at catchment scale, *Water Resour. Res.*, 54, 5856–5877, <https://doi.org/10.1029/2017WR022380>, 2018.
- 710 Yang, X., Jomaa, S., Büttner, O., and Rode, M.: Autotrophic nitrate uptake in river networks: A modeling approach using continuous high-frequency data, *Water Res.*, 157, 258–268, <https://doi.org/10.1016/j.watres.2019.02.059>, 2019a.
- Yang, X., Jomaa, S., and Rode, M.: Sensitivity Analysis of Fully Distributed Parameterization Reveals Insights Into Heterogeneous Catchment Responses for Water Quality Modeling, *Water Resour. Res.*, 55, 10935–10953, <https://doi.org/10.1029/2019WR025575>, 2019b.
- 715 Yang, X., Tetzlaff, D., Soulsby, C., Smith, A., and Borchardt, D.: Catchment Functioning Under Prolonged Drought Stress: Tracer-Aided Ecohydrological Modeling in an Intensively Managed Agricultural Catchment, *Water Resour. Res.*, 57, e2020WR029094, <https://doi.org/10.1029/2020WR029094>, 2021.
- Yang, X., Rode, M., Jomaa, S., Merbach, I., Tetzlaff, D., Soulsby, C., and Borchardt, D.: Functional Multi-Scale Integration of Agricultural Nitrogen-Budgets Into Catchment Water Quality Modeling, *Geophys. Res. Lett.*, 49, e2021GL096833, <https://doi.org/10.1029/2021GL096833>, 2022a.
- 720 Yang, X., Tetzlaff, D., Soulsby, C., and Borchardt, D.: HiWaQ_v1.0: a flexible catchment water quality assessment platform, Zenodo [code], <https://doi.org/10.5281/zenodo.7107394>, 2022b.
- Young, R. A., Onstad, C. A., Bosch, D. D., and Anderson, W. P.: AGNPS: A nonpoint-source pollution model for evaluating agricultural watersheds, *J. Soil Water Conserv.*, 44, 1989.
- 725 Zhi, W., Shi, Y., Wen, H., Saberi, L., Ng, G. H. C., Sadayappan, K., Kerins, D., Stewart, B., and Li, L.: BioRT-Flux-PIHM v1.0: A biogeochemical reactive transport model at the watershed scale, *Geosci. Model Dev.*, 15, 315–333, <https://doi.org/10.5194/gmd-15-315-2022>, 2022.